ICAS Paper No. 70-54

WIND TUNNEL WALL EFFECTS FOR V/STOL AIRPLANES WITH LIFT JETS

by
R. Jenny Dr.ing. and B. Häni, dipl. ing.
ETH, Swiss Federal Aircraft Factory
Emmen, Switzerland

The Seventh Congress of the International Council of the Aeronautical Sciences

CONSIGLIO NAZIONALE DELLE RICERCHE, ROMA, ITALY / SEPTEMBER 14-18, 1970

Price: 400 Lire

WIND-TUNNEL WALL EFFECTS FOR V/STOL AIRPLANES WITH LIFT JETS

*R. Jenny and **B. Häni
Swiss Federal Aircraft Factory, Emmen

Abstract

Lifting an aeroplane by vertically directed jets can lead to severe aerodynamic problems, such as lift loss, loss of stability, hot gas ingestion etc. Extended wind-tunnel testing of such configurations is therefore necessary. Although well established wind-tunnel technics are commonly used, there still remain important questions unclear. Until now, not much quantitative information is available on the importance of wall effects.

Wall interference effects have been computed by using known theoretical models for a jet penetrating vertically into a uniform parallel flow. After minor modifications of one of the jet models, it was possible to study more complex jet arrangements. In some cases, calculated boundary corrections have been compared with measurements in the wind-tunnel.

*Dr. ing., formerly Head of Experimental Section, Research Dept., now President, Tecifor AG.
**Dipl. ing., Engineer, Experimental Section

I. Introduction

According to Ref.[7] a suitable test section for V/STOL aircraft models has an area of about 160 m^2. We believe that valuable testing in smaller wind-tunnels can be made under certain conditions. However, more knowledge about the influence of tunnel boundaries is required to decide if a model of a certain size can be successfully tested. Until now there is only limited information available on the magnitude of wall effects. This paper makes a contribution to this knowledge by studying wind-tunnel wall effects due to jets directed at large angles into a mainflow, e.g. a situation as it is encountered in the transition phase of a V/STOL aircraft with lift jets.

A similar problem of these wall effects occurs when testing aircraft models powered by lift fans or lifting rotors. Heyson[3] has developed a method for evaluating wind-tunnel corrections in such situations. Occasionally, this theory is also applied to provide corrections when testing a model with lift jets. But it is not evident that this potential theory for propellers can

also be used to calculate the effects of high energy lift jets.

Presently there exist some theoretical or semi-empirical methods for describing the interference flow field of a jet in a parallel flow. Two of these are analyzed in the present paper and are then used to determine the wall interference.

II. Mathematical Models

1. Theoretical model I based on a universal jet form

Early attempts to determine analytically the induced flow velocities due to a jet penetrating at a right angle into a homogeneous flow either considered the jet as a semi-infinite rigid cylinder, placed in an inviscid flow, or it used a simple superposition of the parallel flow and an undeflected jet. Both approaches could not describe satisfactorily experimental results. Later it had been noticed that the dominant features of a flow penetrated by a jet are two trailing vorteces on both sides of the jet. These vorteces seem to be primary generators of the induced velocities at large distances from the jet.

Wooler[2] has developed a theory giving the position and strength of the horse shoe vorteces along the jet plume. The geometrical form of the jet centre line is expressed by a universal formula:

$$\frac{x}{d_o} = B(\cosh z/d_o B - 1)$$

where $B = 0{,}19(U_j/U_\infty)^2$

which is obtained empirically. There exist some similar expressions, published by other authors [6] which lead to slightly different results for the jet shape. It was found that these small differences do not strongly affect the results of downwash corrections. It is further assumed that the deflection of the jet is related to a purely inviscid flow mechanism and that the jet momentum flux and the velocity remain constant along the jet path.

From the curvature of the jet the normal force N on a jet element is then obtained by writing the momentum balance:

$$N = \rho A_j U_j^2 ds/R$$

The relation between this force and the circulation of the horse shoe vortex at the jet element is:

$$d_o \rho U_\infty \Gamma' ds = \rho A_j U_j^2 ds/R$$

The two trailing vorteces are assumed to be located at a distance of one half jet diameter $d_o/2$ on both sides of the jet centre line. Their circulation along the jet path is then:

$$\Gamma = \int_o^s \Gamma' ds$$

The total effect of a deflected jet on the mainflow is represented by this vortex system. Magnitude and direction of the jet induced velocities can be calculated at any point.

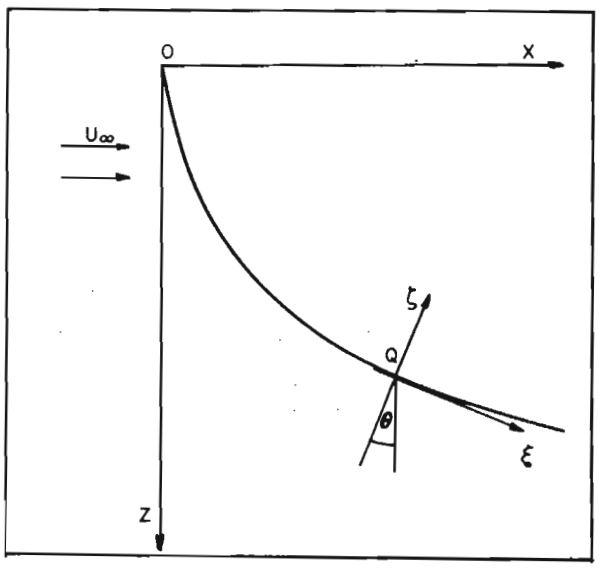

Fig.1 Coordinate System

2. Theoretical model II including jet entrainment

To cope with more general jet configurations, the theoretical model should also comprise of the basic physical mechanism such as entrainment, blocking and vortex effects. This lead us to adopt a model proposed by Wooler, Gallagher and Burghart[1] which is in this respect more complete. For a detailed description of this model reference is made to the author's original paper. Here it is only summarized and more emphasis is put on the modifications that are necessary in our situation.

Considering a jet in a uniform parallel flow a pressure force acts on a jet element. This force per unit length is:

$$N = 0.5\, C_n \rho U_\infty^2 \cos^2\theta\, d$$

It could be interpreted as a normal force due to the crossflow. The coefficient C_n is a constant. Its value of 1.8 is chosen in analogy to the drag coefficient of an elliptical cylinder. In Ref.[1] this force is used to calculate the jet centre line, but it does not contribute to the interference velocities. In our interference model it is related to a vortex system which is assumed to be a horse shoe vortex "bound" to the jet path. Its strength per unit length is given by

$$2\Gamma' = C_n \rho U_\infty^2 \cos^2\theta\, d/\rho U_\infty d_o$$

As will be shown later this effect must be included to obtain the induced far-field correctly.

The jet element also entrains material from the surrounding mainstream by viscous action. This entrained fluid having a momentum in the direction of the mainstream also deflects the jet. In Ref.[1] an expression for the entrainment is given:

$$E = \rho E_1 U_\infty d\cos\theta + \frac{\rho E_2 (U_j - U_\infty \sin\theta) C}{1 + E_3 U_\infty \cos\theta / U_j} \qquad (1)$$

E_1, E_2, E_3 are constants and C is the circumference of the jet. Wooler, Burghart and Gallagher choose:

$$E_1 = 0.35 \quad E_2 = 0.08 \quad E_3 = 30.0$$

The determination of the numerical values for these constants seems to be somewhat hazardous. Therefore the entrainment was measured in our wind-tunnel. Although the experimental method employed must be considered as rather rough, the results correspond to Eq.(1). (See Fig.2). In these experiments a jet emerged through a circular nozzle of 0.1 m diameter with a Mach number of about 0.6 into an open wind-tunnel. The mass flow has been determined by measuring the total pressure just outside the tunnel boundary where the static pressure can be assumed to be constant and the flow direction parallel to the jet flow. The distance between jet exit and the wind-tunnel boundary as well as the angle between the nozzle axis and the main-flow direction have been varied (s = 200 and 500 mm, $\theta_o = 0^o$ and 30^o). Measurements were also made with an oval-shaped nozzle with the same exit cross section. In Fig.2 the entrainments obtained are plotted and compared to the values calculated with the aid of Eq.(1).

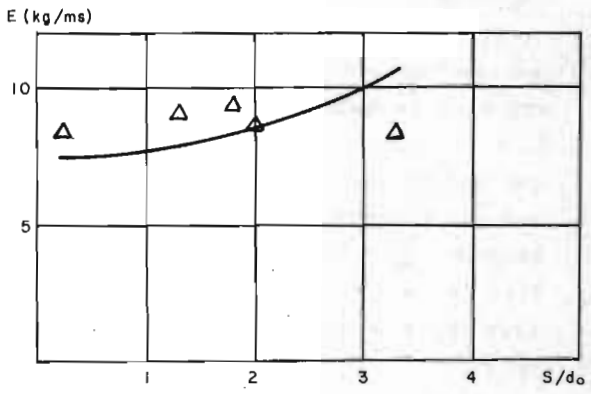

Fig.2 Entrained fluid of a jet (m = 8)

—— calculated by Eq.(1)
Δ measured points

Writing now the continuity and momentum equations for a jet element, one obtains:

$$\rho(d/ds)(A_j U_j) = E \qquad (2)$$

$$\rho(d/ds)(A_j U_j)^2 = EU_\infty \sin\Theta \qquad (3)$$

$$\rho A_j U_j^2/R = EU_\infty \cos\Theta + 0.5 C_n \rho U_\infty^2 \cos^2\Theta \qquad (4)$$

Observation of the development of the jet cross-section suggests that for

$$0 < (z/d_o)(U_\infty/U_{jo}) < 0.3$$

the section is elliptical with a ratio of minor to major axis linearly decreasing from 1 at jet exit to 1/4 at:

$$z/do = 0.3 U_{jo}/U_j$$

For cross-sections further downstream this ratio remains constant = 1/4. The integration of Eqs. (2), (3), (4) yields the jet shape.

The interference velocities produced by the entrainment are simulated by singularities (sinks). In this theoretical model the total interference effects are a superposition of the effects of the vorteces and sinks.

3. Comparison of the theoretical and experimental interference field

Figs. (3), (4) and (5) show the measured near-field downwash angles. They are compared with the predictions of the theoretical models outlined above. The flow angles have been measured at an arbitrary position somewhat downstream from the jet exit on a line extending in the y-direction. The mutual agreement of the two theories and their agreement with the measurement is evident. To determine which of the two theories gives the best results a more sensitive experimental method would have to be applied.

Figs. (6), (7) and (8) show again downwash angles of the near-field but on vertical lines passing through the jet. Outside the jet boundaries the flow angles are computed by model II. Inside the jet boundaries the flow is calculated from Eqs. (2), (3) and (4). The experimental points are taken from measurements by Jordinson[4].

Fig.3

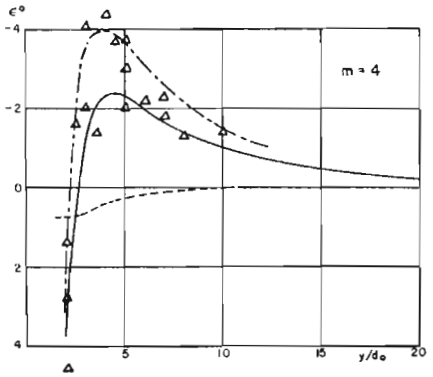

Fig.4

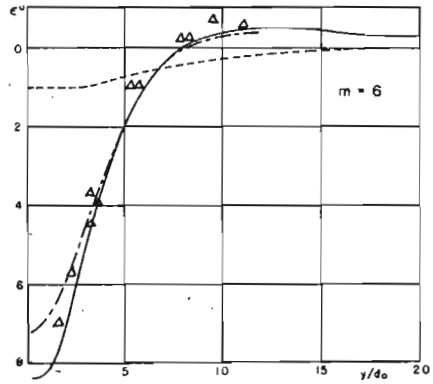

Fig.5

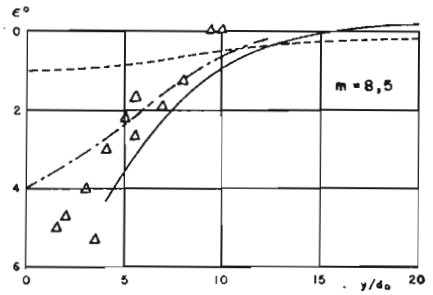

Near-field downwash angles

—·—·— model I

——— model II

----- sinks only

Δ measurements

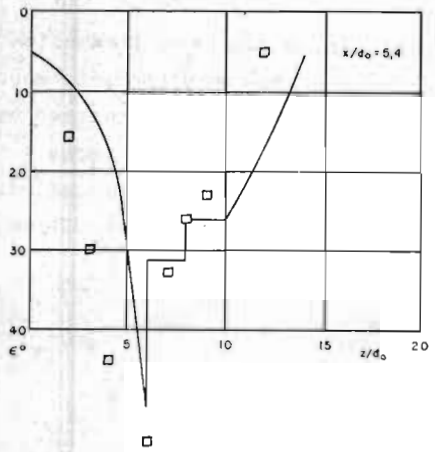

Fig.6

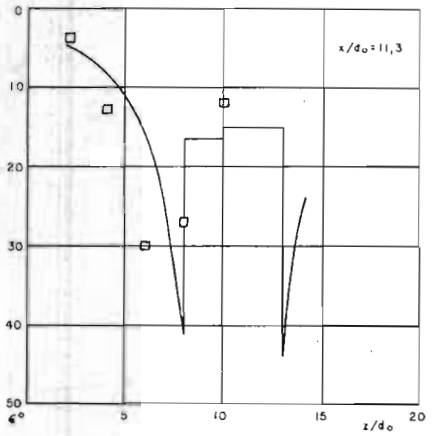

Fig.7

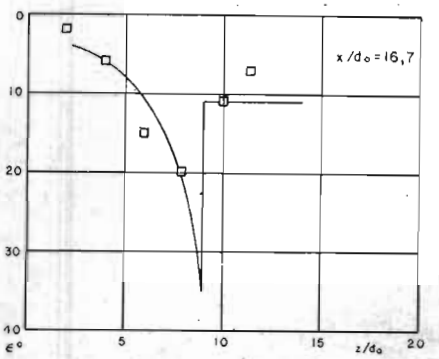

Fig.8

4. Extension of model II

Fig.(9) shows a jet in a three dimensional non uniform cross flow U (U_x,U_y,U_z). The origin of the coordinate system coincides with the jet exit. The x-axis points in the general flow direction while the z-axis is vertical. Let us consider a jet element of length ds in the point Q of the jet centre line. The ξ-axis of the coordinate system ξ,η,ζ coincides with the jet centre line and the η-axis remains parallel to the xy-plane.

Limiting us to small velocity components U_y and small dy/ds the equations of motion may be simplified to become:

$$\rho(d/ds)(A_j U_j^2) \simeq EU_{xz}\sin\alpha \qquad (6)$$

$$\rho A_j U_j^2/R_{xz} \simeq EU_{xz}\cos\alpha + 0.5\, C_n \rho U_{xz}\cos^2\alpha \qquad (7)$$

$$\rho A_j U_j^2/R_{xy} \simeq E(U_y - U_{xz}\sin\alpha\sin(dy/ds)) + 0.5\, C_n \rho (U_y - U_{xz}\sin\alpha\sin(\frac{dy}{ds}))^2 d \qquad (8)$$

where $\alpha = \varepsilon + \Theta$

$$E = \rho E_1 U_{xz} d\cos\alpha + \frac{\rho E_2 (U_j - U_{xz}\sin\alpha)C}{1 + E_3 U_{xz}\cos\alpha/U_j} \qquad (9)$$

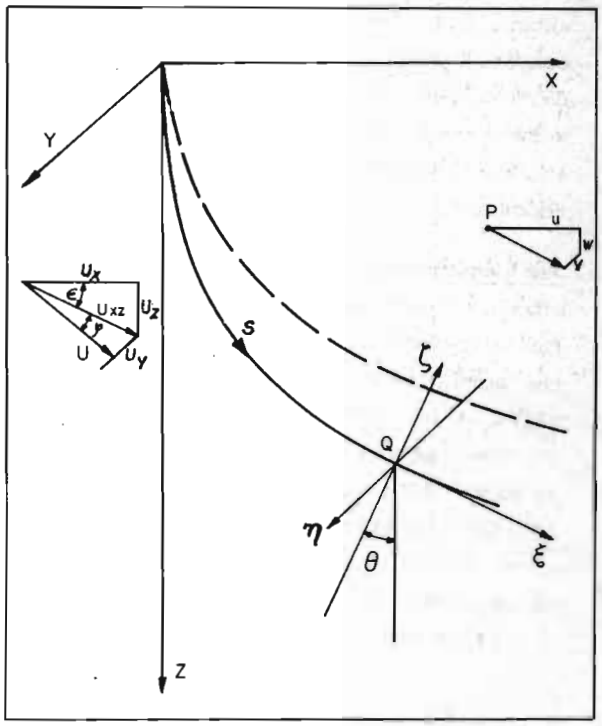

Fig.9 Coordinate systems

The integration of the equations of motion is made, assuming that the development of the jet cross-section is the same as in the case of a parallel-flow.

The calculations of the shapes of more than one jet are performed in an iterative manner. Assuming two jets, the first is computed as if it were in a parallel cross

flow. The induced velocities of this jet added to the parallel flow, become the incident flow of the next jet. So this one can be computed and its interference velocities are added to the oncoming flow of the first jet which in the next step will be recalculated. The iterations are continued until the variations of consecutively calculated jets become neglegible. In most cases this is achieved after two or three iterations. The analogue procedure is applied to get the shapes of more than two jets.

In Fig.(10) a photograph of the smoke plume of a configuration of three jets is shown. Calculations of the centre line are compared with a photographed jet. The obtained centre lines agree well with the observed ones. The photograph also visualizes the configuration of the two trailing vorteces along both sides of each jet.

Jet penetration. The main difficulty occurs when one jet penetrates another. Although the mathematical model does not describe the actual mechanics of shear flow accurately, it has also been used to calculate the jet path through the penetration zone. In many cases of practical interest the jets do not have equal dimensions at the crossing point. The problem may therefore be separated into two cases which both can be calculated with the aid of model II.

1. The jet to be calculated penetrates a wider jet.
2. The jet to be calculated circumflows a smaller jet.

1. The section fo the smaller jet laying inside the wider jet is assumed to behave as in the case of a parallel flow with the velocity and direction of the circumflowing jet. Its centre line in the crossing region is calculated from the equations (2), (6), (7), (8), (9) substituting U_{xz} by the jet velocity of the circumflowing jet.

2. The circumflowing jet itself experiences the reactions of the smaller jet. Basically these reactions are generated by the singularities (sinks, vorteces) according to the theoretical model. In this simple analysis the three-dimensional

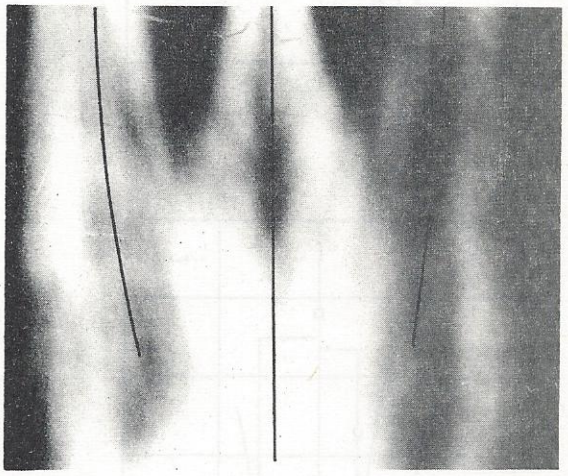

Fig.10 Configuration of 3 jets viewed vertically to the mainstream.

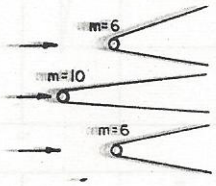

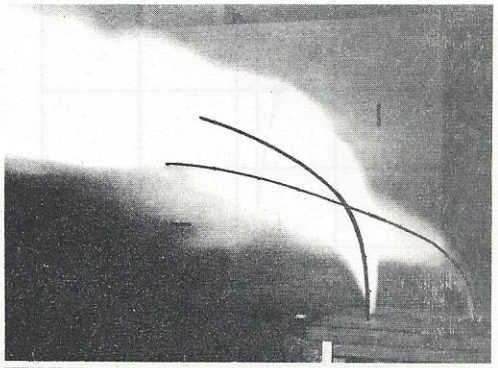

Fig.11

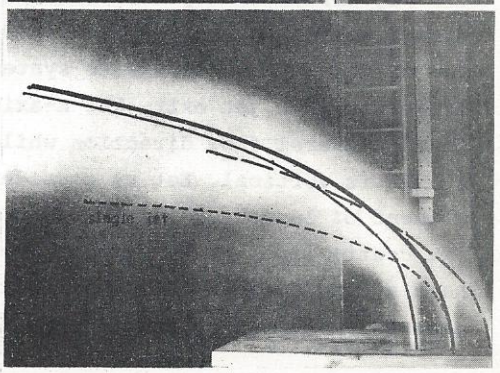

Fig.12

flow distortion cannot be taken into account, but it was assumed that the hypothetical centre line of the circumflowing jet deviates corresponding to its momentum and mass flux change as given by the following equations:

$$\rho(d/ds)(A_j U_j)_1 = - E_2$$

$$\rho(d/ds)(A_j U_j^2)_1 = - E_2 U_{j1} \sin\alpha - 0.5\, C_n \rho U_{j1}^2 \cos^3\alpha d_2$$

$$\rho(A_j U_j^2)_1 / R_1 = - 0.5\, C_n \rho U_{j1}^2 \cos^2\alpha \sin\alpha d_2$$

Subscribt 1 designs the circumflowing jet, subscribt 2 the penetrating one.

Additionally the outer flow acts on the penetration zone as a whole. Its effects i.e. momentum and mass flux contribution, are distributed on the individual jets according to their spatial share of the penetration region. This is achieved by introducing a factor $q = \sqrt{d_1^2 + d_2^2}\,/(d_1 + d_2)$ into Eqs.(2), (6), (7), (8), (9). In this way the individuality of the jets can be preserved which is necessary to allow the jets to separate again after the crossing process. In an analogous way this theory can be extended to the penetration of more than two jets.

In Fig.(11) an arrangement of two jets one behind the other is shown. A jet with initial velocity ratio m = 10 is penetrating one with m = 6 exhausting in a distance of 10 d_o upstream. The calculated jet paths agree well with experimental ones.

The interaction of three jets with equal momentum flux m = 6 are shown in Fig.(12). The distance between the nozzles is 3 d_o. Having a very big extent of "penetration zone" the mutual interaction of the three jets is considerable. The development of the path of an undeflected jet with the same momentum flux is also marked.

III. Wall Effects

1. Single jet

In the previous sections it has been shown that there exist mathematical models which describe jet paths and the interference flow pattern rather closely. Using the classical method of images the effects of various tunnel boundaries can be calculated.

Considering a single jet beginning in the center of a rectangular wind-tunnel with closed boundaries the corresponding image jets must be arranged as shown in Fig.(13) to produce a flow surface matching the tunnel boundaries. The wall effects may be interpreted as the flow field of these "image jets". In an analogous way the effects of an open tunnel boundary are obtained.

Fig.(14) shows the wall induced downwash angles (δ = arc tgw/U_∞) at the centre of a closed and open test section for a single jet exhausting at the centre of the wind-tunnel. The different lines plotted correspond to different velocity ratios $m = U_j/U_\infty$. These results are obtained by using the jet model I. The comparison with analogous results of the theory II is shown in Fig.(15). The downwash predictions of theory I exceed the results of theory II.

In Fig.(16) the tunnel boundary interference calculated according to the original model of Ref.[1] is compared with that of model II. It operates with a distribution of sinks and doublets. Its wall effects seem to be too small considering our experimental investigations which which are described below.

We tried to verify these wall effects experimentally. As they are relatively small the test arrangement had to be chosen very carefully to yield results with the required accuracy. Instead of measuring the tunnel boundary effects themselves it was

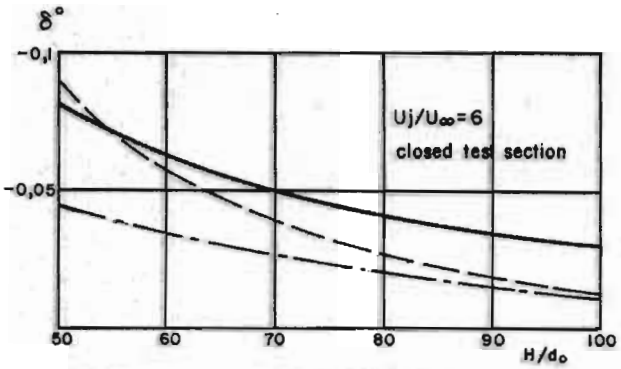

Fig.16

—— model II
—·— sinks and doublets
— — doublets only

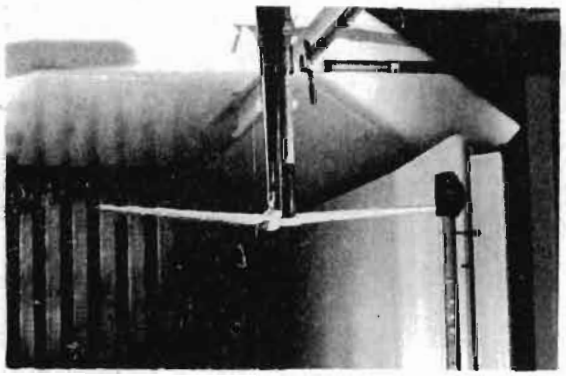

Fig.17 Test arrangement

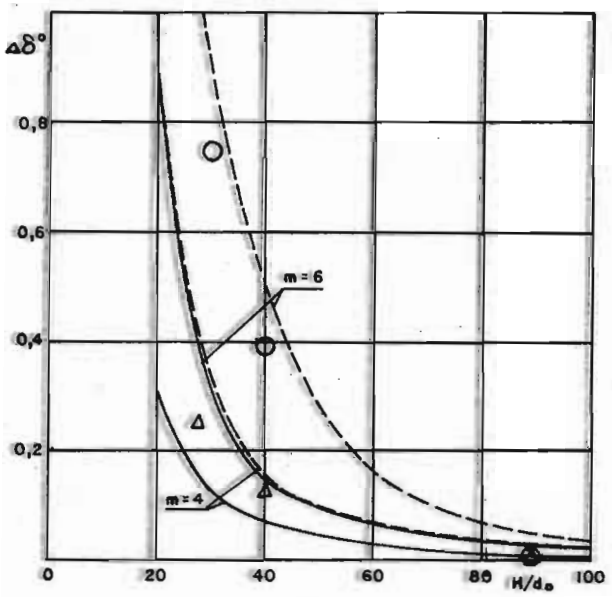

Fig.18 Difference of wall effects between an open test-section and a test-section with a bottom.

—·— model I
—— model II

believed sufficient to measure the difference between the effects of an open test section and a test section with a bottom only. This allowed a quick and simple change of the tunnel configuration which could be performed without disturbing the running conditions of the jet and wind-tunnel. Fig.(17) shows the test arrangement. A single jet with exchangeable nozzles of different diameters is mounted in the centre of an open test section. The air is supplied through a vertical pipe from a compressor. At some jet diameters downstream there is a wing mounted on a balance. By measuring the lift with and without tunnel ground-board, an average downwash angle due to altered wind-tunnel boundaries can be determined.

In Fig.(18) these experimental results are compared with the corresponding theoretical predictions of the two models. If we take into account the accuracy of the experimental points, they do not contradict either of the two theoretical models, although the results of model I seem to fit better to the experimental results. There exists a certain difference between the results from model II and those that were obtained experimentally. Model II would permit an adjustment within certain limits e.g. a small diminution of the rather roughly determined entrainment yields relatively large wall interferences, because in Eq.(7) a smaller E demands a bigger C_n to give the same jet path. This would cause an increase of the circulation Γ which would together with an attenuation of sinks intensify the wall effects and reduce the difference to the experimental points. See Fig.(16). Also a certain blockage effect could be taken into account. We do not believe that an adjustment of model II should be based only on these measurements. More experimental data with higher accuracy must be available. Actually we are developing a new system to measure flow angles

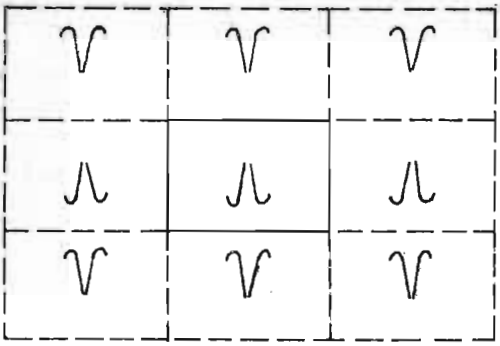

Fig.13

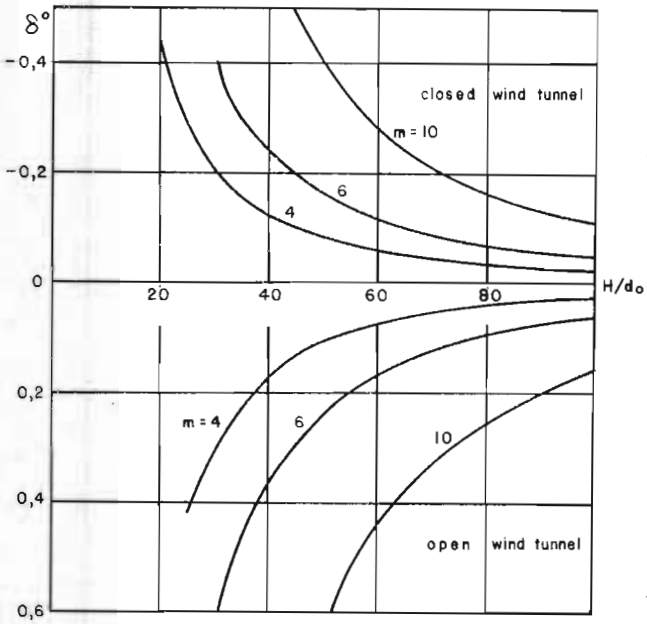

Fig.14 Wall effects (model I)

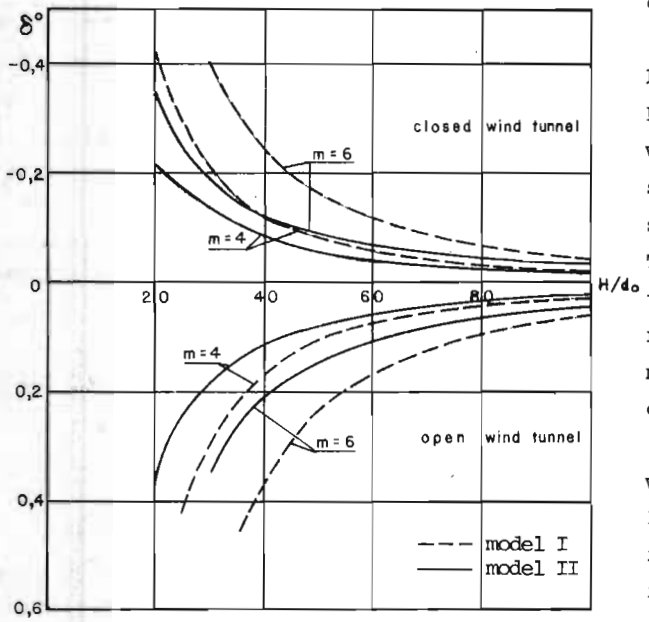

Fig.15 Wall effects

with much more precision.

At the moment the wall effects of a single jet may be calculated using the first theory. It does not only seem to yield results closer to the experiments but it is also simpler in its application.

2. Multiple jet configuration

Wind-tunnel tests with single jet configurations are of rather limited interest because most of the V/STOL designs use several lift engines or at least several distinct lift jets. If no significant interaction occurs between the different jets or between the jets and the tunnel boundaries, the wall effects can be calculated by superimposing the effects of single jets obtained by the theory outlined above. If interactions are important the wall effects calculated in this way must be considered as rough approximations. As explained in part (II.2.) only the model II can represent mutual interactions of the different jets. Although no satisfactory experimental verification of model II could be achieved to date, it is applied to study the effects of the mutual interactions between the jets on the wall interferences.

The three examples of part (II.4.) (see Figs.(6), (7), (8)) are considered. Figs.(19), (20) and (21) show the calculated wall effects. They are compared with a simple superposition of the effects of single jets neglecting mutual interaction. The simple superposition of the effects of two individual jets leads to about the same results as a computation that considers the mutual influence; in case 1 as well as in case 2.

But in the third case (see Fig.(12)) where three jets exhaust in a distance of $3d_o$ one behind the other, the interaction is essential and therefore the wall effects in Fig.(21) are different.

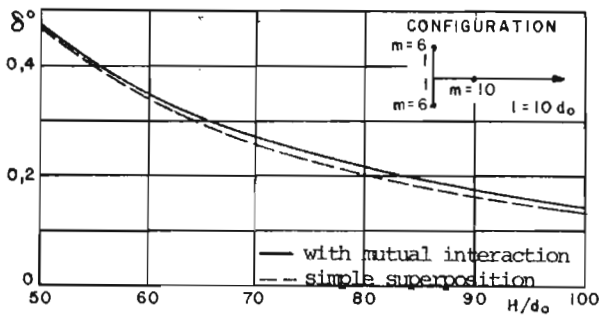

Fig.19 Wall interference

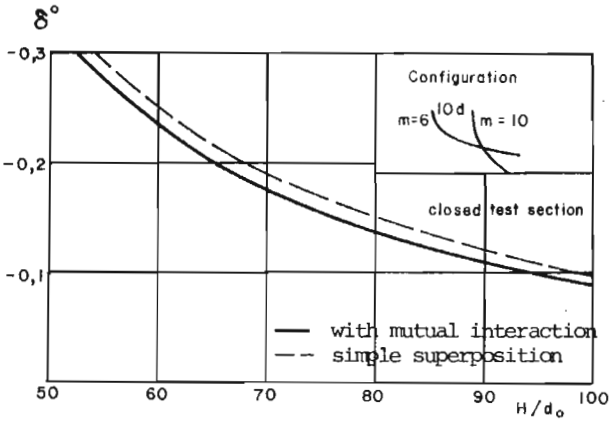

Fig.20 Wall interference

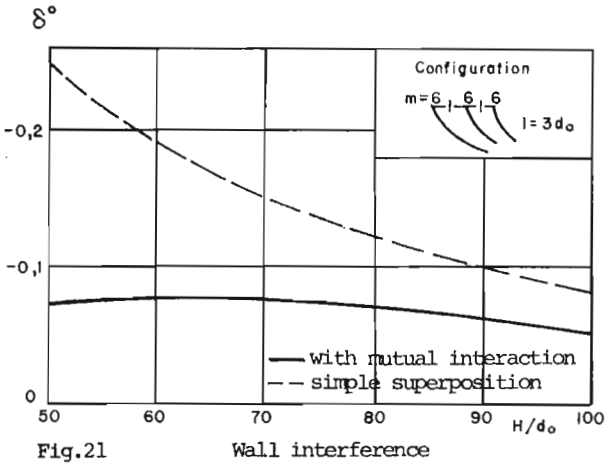

Fig.21 Wall interference

IV. Conclusion

Wall effects for lift jets have been calculated with two different theoretical models.

A comparison of the theoretical predictions with experimental wall effect measurements seem to indicate that the simple model I simulates the far-field of the jet interference better than the more elaborate model II.

By modifying the entrainment constants in model II and including a blocking effect of the jet, the far-field simulation could be improved.

By generalizing the second model jet arrangements with mutual jet interactions can be calculated.

It was found that in many practically important configurations a superposition of the wall effects of single jets is sufficient.

V. Nomenclature

a	ratio minor axis to major axis of elliptical cross section
A_j	jet cross-sectional area
C	circumference of jet cross section
C_n	load coefficient
d	diameter of circular jet cross section or length of major axis of elliptical jet cross section
E	jet entrainment
E_1, E_2, E_3	entrainment coefficients
m	velocity ratio
N	normal force on a jet element
R	local jet radius of curvature
s	coordinate along jet centre line
U	undisturbed mainstream speed
U_j	local jet speed
u,v,w	induced velocities in the X,Y,Z-direction
Θ, ε	angles defined in Fig.(1) and (9)
α	$\Theta + \varepsilon$
ρ	density of jet and mainstream fluid
Γ	circulation of trailing vorteces
Γ'	circulation per unit length

Subscribts

o conditions at the jet exit

∞ conditions at infinity

VI. References

(1) P.T. Wooler, G.H. Burghart and J.T. Gallagher
Pressure Distribution on a Rectangular Wing with Jet Exhausting Normally into an Airstream.
J. Aircraft VOL 4 No 6 Nov. - Dec.1967

(2) P.T. Wooler
On the Flow Past a Circular Jet Exhausting at Right Angles from a flat Plate or Wing
IARD, Vol. 71, March 1967

(3) H.H. Heyson
Linearized Theory of Wind Tunnel Jet-Boundary Corrections and Ground Effect for VTOL - STOL Aircraft
NASA TR R - 124, 1962

(4) R. Jordinson
Flow in a Jet Directed Normal to the Wind
R&M No. 3074
A.R.C. Technical Report

(5) J.F. Keffer - W.D. Baines
The round turbulent jet in a cross-wind
J.Fl. Mech. 15 (1963)

(6) G.N. Abramovich
The Theory of Turbulent Jets.
M.I.T. Press, Cambridge

(7) M.P. Knowlton
A Study of V/STOL
Aerodynamic Test Facilities
Dept. of Aerospace and Mechanical Science
Princeton University 1964